The current issue and full text archive of this journal is available at
www.emeraldinsight.com/0264-4401.htm

Topology optimization of bi-modulus structures using the concept of bone remodeling

Kun Cai
College of Water Resources and Architectural Engineering, Northwest A&F University, Yangling, China
Zhen Luo
School of Electrical, Mechanical and Mechatronic Systems, University of Technology, Sydney, Australia, and
Qing H. Qin
School of Engineering, Australian National University, Canberra, Australia

Received 12 May 2013
Revised 16 November 2013
Accepted 18 November 2013

Abstract

Purpose – The purpose of this paper is to develop a heuristic method for topology optimization of a continuum with bi-modulus material which is frequently occurred in practical engineering.

Design/methodology/approach – The essentials of this model are as follows: First, the original bi-modulus is replaced with two isotropic materials to simplify structural analysis. Second, the stress filed is adopted to calculate the effective strain energy densities (SED) of elements. Third, a floating reference interval of SED is defined and updated by active constraint. Fourth, the elastic modulus of an element is updated according to its principal stresses. Final, the design variables are updated by comparing the local effective SEDs and the current reference interval of SED.

Findings – Numerical examples show that the ratio between the tension modulus and the compression modulus of the bi-modulus material in a structure has a significant effect on the final topology design, which is different from that in the same structure with isotropic material. In the optimal structure, it can be found that the material points with the higher modulus are reserved as much as possible. When the ratio is far more than unity, the material can be considered as tension-only material. If the ratio is far less than unity, the material can be considered as compression-only material. As a result, the topology optimization of continuum structures with tension-only or compression-only materials can also be solved by the proposed method.

Originality/value – The value of this paper is twofold: the bi-modulus material layout optimization in a continuum can be solved by the method proposed in this paper, and the layout difference between the structure with bi-modulus material and the same structure but with isotropic material shows that traditional topology optimization result could not be suitable for a real bi-modulus layout design project.

Keywords Topology optimization, Bi-modulus structures, Bone remodelling, Material replacement, Reference interval

Paper type Research paper

1. Introduction

Structural optimization of size, shape and topology is becoming essential in the design process of structures due to the rapid development of computational techniques (Eschenauer and Olhoff, 2001). Optimizing topology of a continuum structure is one of

This research is partially supported by the National Natural-Science-Foundation-of-China (No. 50908190) and the Youth Talents Foundation of Northwest A & F University (No. Z111020903) and Research Foundation (No. GZ1205) of State Key Laboratory of Structural Analysis for Industrial Equipment, Dalian University of Technology, Dalian, PR China.

Engineering Computations: International Journal for Computer-Aided Engineering and Software
Vol. 31 No. 7, 2014
pp. 1361-1378

0264-4401
DOI 10.1108/EC-05-2013-0128

the most challenging tasks in the structural optimization. Topology optimization consists of a numerical procedure to iteratively re-distribute a given amount of material, so as to automatically determine the optimal connectivity of material layout in the reference domain subject to supports and loads. The optimum of the design can be obtained when the prescribed objective function is minimized or maximized under specific constraints. Over the past two decades, topology optimization has experienced considerable development with several typical methods for a broad range of areas, such as the homogenization method (Bendsøe and Kikuchi, 1988), solid isotropic microstructures with penalization (SIMP) method (Zhou and Rozvany, 1991; Bendsøe and Sigmund, 1999; Qin and He, 2005), evolutionary structural optimization (ESO) method (Xie and Steven, 1993) and level set method (Wang *et al.*, 2003; Allaire *et al.*, 2004; Luo *et al.*, 2008, 2009).

However, it is found that the structures with bi-modulus materials are relatively seldom studied in the area of topology optimization. Bi-modulus structures, in which the tensile modulus is not equal to the compressive one in a given direction, widely exist in engineering, such as the concrete in civil engineering or cast iron in mechanical engineering. So far only a limited number of research efforts were applied to structures consisting of material with different tensile and compressive moduli (Chang *et al.*, 2007). For most topology optimization methods, mechanical properties of bi-modulus structures should be considered as nonlinear (Chang *et al.*, 2007), which will make the computational cost expensive in numerical analysis iteratively in order to find an acceptable displacement field to update design variables. To reduce the computational time, a heuristic method is proposed in this paper based on the concept of bone remodeling technique (Wolff, 1986; Cowin, 1986; Qin and Ye, 2004; Qu *et al.*, 2006; Cai *et al.*, 2008a, b).

In bone mechanics, Wolff's Law (Wolff, 1986), proposed by the German physiologist Julius Wolff in 1892 and now widely accepted in the field of biomedical engineering, states that bone has an ability to change its size, shape and structure via bone apposition and absorption to adapt environmental changes, including mechanical loadings. This phenomenon is called as bone remodeling (Cowin, 1986; Fernandes *et al.*, 2002; Qin *et al.*, 2005; Qu and Qin, 2006; Qin, 2007). Researchers also considered the bone remodeling to be a kind of optimization process (Mullender *et al.*, 1994; Fernandes *et al.*, 1999; Bagge, 2000; Andrade-Campos *et al.*, 2012), as bone distributes in a way that maximizes its stiffness in nature, while the trabeculae will orient along higher principal stress lines. As a consequence, the rule of bone remodeling can be used as a tool for topology optimization of continuum structures (Harrigan and Hamilton, 1994; Jang and Kim, 2008; Cai *et al.*, 2008a, b). Jang *et al.* (2009) showed the equivalence between analogies of strain energy density based bone-remodeling algorithm and topology optimization of structures. In the work of Cai *et al.* (2008a), the material in topology optimization is defined as a bionic material with different reference interval of strains under tension or compression. But the material is still isotropic. The final difference of material properties only means the growth condition (remodeling) of material under tension and is not identical to that under compression. Cai and Shi (2010) suggested reference interval method to solve layout optimization with tension/compression only material, which replace the original tension/compression material with an isotropic material and then the design variables were updated according to reference interval of the strain energy density.

However, bi-modulus material is stress dependent and different from tension/compression only material. Using the material replacement method (Cai *et al.*, 2008b) to

simplify analysis of structures with bi-modulus material, the original bi-modulus material should be replaced with at least two isotropic materials. Therefore, both of elastic modulus and relative density of a finite element in the design domain should be updated, simultaneously. They are the main differences between the present work and that from Cai *et al.* (2008b).

In the present method, a heuristic approach is proposed for the topology optimization of continuum structures with bi-modulus material. The original structural optimization is considered as a bone remodeling process under the same loading and boundary conditions. The update of design variables is determined by the comparison between the local strain energy densities (SED) and the reference interval of SED which is corresponding to the lazy zone (Huiskes *et al.*, 2000) in bone mechanics. The original bi-modulus material is replaced with two types of solid isotropic materials, in which the moduli are equal to the tensile and compressive moduli, respectively. In the optimization process, elastic modulus of an element is updated according to the principal stresses, and the relative density is updated according to the effective strain energy density. The topology will also be expressed as the layout of relative densities of finite elements. In this work, penalization law between porosity and elasticity of elements is adopted to reduce the amount of elements with mid-densities to give an approximated binary design. Therefore, the present method combines the concept of the ESO method to update design variables and SIMP method to express the relations between porosity and elasticity.

2. Bi-modulus materials

When the tensile modulus (E_T) and compression modulus (E_C) of a material in a direction are distinct, the material is called as bi-modulus material. For illustration, the stress-strain (σ-ε) curve of a typical bi-modulus material is shown in Figure 1(a). In particular, the bi-modulus material will be tension-only material when $\alpha = 0$ or compression-only material when $\beta = 0$. The curve in Figure 1(b) shows an isotropic bi-modulus material with different tension/compression strength, e.g. $\sigma_T \neq \sigma_C$.

Traditionally, topology optimization is formulated as a material distribution problem in which solid material and void regions are described by discrete density values 1 and 0, respectively. To overcome the difficulty of NP-hard problem of discrete

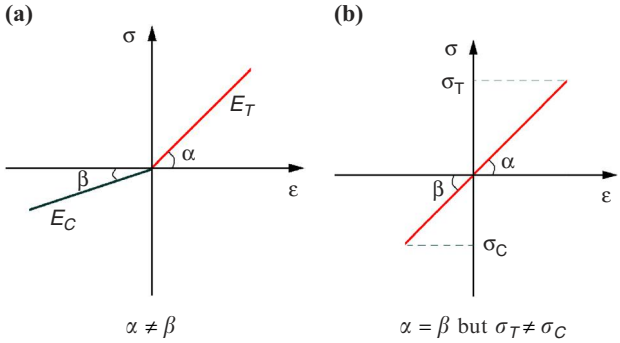

Notes: (a) Bi-modulus material; (b) isotropic material with different tensile/compressive strength

Figure 1.
Two types of stress-strain (σ-ε) curves

optimization (Gao, 2007; Gao and Ruan, 2010), the topology optimization problem is relaxed to enable discrete density variables take intermediate values as continuous variables inside the interval [0, 1]. Consequently, the material properties will be continuously dependent on the local amount of material. In this work, a power-law relationship based on the standard SIMP is used to penalize intermediate densities (Bendsøe and Sigmund, 1999).

At any point of the design domain Ω, the stiffness tensor is given as follows:

$$D_{m,\,ijkl} = \rho_m^p D_{0,\,ijkl} \tag{1}$$

where "m" represents any material point in the design domain, $\rho_m \in [\delta, 1.0]$ is the relative density of the mth material point. δ is a very small positive number used to avoid numerical singularity in the finite element method. The power p is the penalization factor, to penalize intermediate variables to make the relaxed design close to the binary (0 and 1) one as much as possible. In this study $p \geqslant 2$ is used (Bendsøe and Sigmund, 1999). $D_{m,ijkl}$ is the stiffness tensor of the mth material point and $D_{0,ijkl}$ is the stiffness tensor of the solid material (i.e. the relative density is 1) which is not limited to isotropic material.

When the solid material is isotropic, $D_{0,\,ijkl}$ in Equation (1) can be degenerated to the following:

$$D_{0,\,ijkl} = \lambda\, \delta_{ij}\delta_{kl} + \mu\left(\delta_{ik}\,\delta_{jl} + \delta_{il}\,\delta_{jk}\right) \tag{2}$$

where δ_{ij} is the Kronecker delta. λ and μ are two Lame constants of the solid material.

3. Methods of topology optimization

3.1 Basic equations of linear elasticity problems

For linear elastic structures, the basic equations and boundary conditions are written as follows:

$$\begin{aligned} &\sigma_{ij} = D_{ijkl} : \varepsilon_{kl} \\ &\varepsilon_{ij} = \frac{1}{2}\left(v_{i,j} + v_{j,i}\right) \\ &\sigma_{ij,i} + f_j = 0 \end{aligned} \tag{3}$$

$$\begin{aligned} &\Gamma_\sigma : \quad \sigma_{ij} \cdot n_j = F_i^* \\ &\Gamma_v : \quad v_i = v_i^* \\ &\Gamma_\sigma + \Gamma_v = \partial\Omega \end{aligned} \tag{4}$$

where σ_{ij} is the stress tensor, ε_{ij} the strain tensor, v_i the displacement vector of a point, f_i the body force vector, F_i^* the boundary force on the boundary Γ_σ of solution domain Ω, with the normal outward direction n_j, v_i^* the assigned displacement on the boundary Γ_v. In our analysis, the well-established finite element method (Qin, 2003, 2005; Qin and Wang, 2008) is adopted to solve the boundary value problems (3) and (4).

3.2 Optimization model for structural stiffness designs

In the optimization, the concept of relative density of a material point in the design domain is considered as design variables. The formulation of the heuristic approach is defined as:

$$\begin{aligned} &\text{Find} \qquad \{\ \rho_m | m \in \Omega\ \}\ \ \&\ \ \left[u_{\inf}^{\infty},\quad u_{\sup}^{\infty}\right] \\ &\text{to satisfy} \quad \begin{cases} \forall u_m^{effective} \in \left[u_{\inf}^{\infty},\quad u_{\sup}^{\infty}\right] \\ \text{or} \quad \rho_m = \begin{cases} 1, & \text{if } u_m^{effective} > u_{\sup}^{\infty} \\ \delta, & \text{if } u_m^{effective} < u_{\inf}^{\infty} \end{cases} \end{cases} \\ &\text{subject to} \quad \phi_i(\{\rho_m\}) \leqslant 0, \quad (i = 1, 2, \cdots, I) \\ &\qquad\qquad \delta \leqslant \rho_m \leqslant 1.0 \end{aligned} \tag{5}$$

where ρ_m is the relative density (the design variable at the mth material point in the design domain). $[u_{\inf}^{\infty},\quad u_{\sup}^{\infty}]$ is the final interval of reference SED. $u_m^{effective}$ is the local effective SED at the mth material point. ϕ_i is the constraint function and I is the maximum number of constraints.

The aim of a stiffness design is to find the optimal material distribution to satisfy the specified constraints. Therefore, the iteration is controlled by active constraints in the optimization. For example, if a volume constraint is active, the objective of optimization can be considered to minimize the structural compliance, or if the active constraint is a displacement constraint, the objective is equivalent to minimize the material volume.

3.3 Material replacement and elastic modulus update

In general, FEM is not very efficient for analyzing structures with bi-modulus material (Medri, 1982). To overcome this, the original material in the design domain is replaced with two types of isotropic porous materials in which the tensile and compressive moduli are set to be identical, respectively. In this case, the material modulus at a point (e.g. m) in the design domain will depend on the stress state at that point. For example, the isotropic material with tensile modulus is used when all of the principal stresses are not negative, e.g. $\sigma_3 \geqslant 0$. The isotropic material with compressive modulus should be adopted when all the principal stresses are not positive, e.g. $\sigma_1 \leqslant 0$. If the first principal stress is positive and the third is negative, namely, the material is under complex stress state and the actual elasticity of bi-modulus material shows orthotropic. It should be mentioned that structural analysis is required to obtain the accurate stress state and to determine material modulus. Here the modulus of an element under complex stress state is set to be the higher one of the two moduli of bi-modulus material. Therefore, the modulus selection can be operated according to the following scheme:

$$E_m = \begin{cases} E_T & \textit{for} \quad \sigma_3 \geqslant 0 \\ \max(E_T, E_C) & \textit{for} \quad \sigma_1 \cdot \sigma_3 < 0 \\ E_C & \textit{for} \quad \sigma_1 \leqslant 0 \end{cases} \tag{6}$$

3.4 Local effective SED

To simplify structural analysis and reduce computational cost, the original (bi-modulus) material is replaced with the stiffer isotropic material. Therefore, only the approximate strain and stress field of the original structure can be found in each loop of structural analysis. It is known that most material in the final optimal structure is under simple stress state. So the approximate stress field tends to be identical to the actual one after several iterations. At the same time, the accurate stress field is unnecessary for the update of the design variables in iteration process in the present approach. To reflect the error between the current stress field and the accurate one, a so-called local effective SED is defined and calculated from the approximate stress state for the update of design variables.

For the mth material point under complex stress state at the kth iteration, the local effective SED can be expressed as follows:

$$u_{k,m}^{effective} = \sum_{i=1}^{3} \frac{1}{2} \mathrm{Sign}(\sigma_i) \cdot \sigma_i \cdot \varepsilon_i \tag{7}$$

where:

$$\mathrm{sign}(\sigma_i) = \begin{cases} 1, & \text{if } \sigma_1 \leqslant 0 \quad \text{or} \quad \sigma_3 \geqslant 0 \\ R_{TCE}^{\omega} = \left(\frac{E_T}{E_C}\right)^{\omega} & \text{if } \sigma_1 > 0 \quad \text{and} \quad \sigma_3 < 0 \end{cases} \tag{8a}$$

$$\omega = \begin{cases} 1 & \text{if } R_{TCE} < 1 \quad \text{and} \quad \sigma_i > 0 \\ 0 & \text{others} \\ -1 & \text{if } R_{TCE} > 1 \quad \text{and} \quad \sigma_i < 0 \end{cases} \tag{8b}$$

where σ_i and ε_i ($i = 1, 2, 3$) are the principal stresses and strains at the mth material point. E_T and E_C are the tensile and compressive moduli of the original bi-modulus material, respectively.

Obviously, Equation (8a) implies that the material shows isotropic when $R_{TCE} = 1$. If $0 < R_{TCE} << 1.0$ (far less than unity), the material can be considered (approximately) as compression-only material. Conversely, the material can be considered as tension-only material when $R_{TCE} >> 1.0$. It should be pointed out that the effective SED at a material point is equal to the actual SED at that point under stress state of either pure tension ($\sigma - \tau$_A circle in Figure 2) or pure compression ($\sigma - \tau$_D circle in

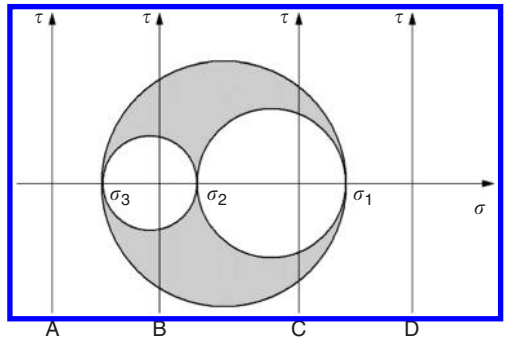

Figure 2.
Mohr's stress circle

Figure 2). Under complex stress states (See $\sigma-\tau$_B or $\sigma-\tau$_C circle in Figure 2), the effective SED are not equal to the actual SED whether the second principal stress, i.e. σ_2, is positive or not.

3.5 Update rule of design variables

After obtaining the local effective SED at any material point, design variables (relative densities) can be updated if the local effective SED falls in the boundaries of the current interval of the reference SED, i.e. $[u_{\inf}^{ref(k)},\ u_{\sup}^{ref(k)}]$, which corresponds to the dead zone or lazy zone of bone remodeling (Huiskes *et al.*, 2000). The increment of the relative density is positive if the local effective SED is greater than the higher bound of the reference interval or negative if the local effective SED is less than the lower bound of the reference interval. Otherwise, the increment of the design variable is set to zero.

Mathematically, the update of relative density at mth material point in the kth step is expressed as:

$$\Delta\rho_{k,m} = \begin{cases} g_1 > 0 & \text{if} \quad u_{k,m}^{effective} > u_{\sup}^{ref(k)} \\ 0 & \text{others} \\ -g_2 < 0 & \text{if} \quad u_{k,m}^{effective} < u_{\inf}^{ref(k)} \end{cases} \tag{9}$$

$$\rho_{k+1,m} = \begin{cases} 1.0, & \text{if} \quad (\rho_{i,k,m} + \Delta\rho_{k,m}) \geqslant 1.0 \\ \rho_{k,m} + \Delta\rho_{k,m} & \text{others} \\ \delta, & \text{if} \quad (\rho_{i,k,m} + \Delta\rho_{k,m}) \leqslant \delta \end{cases} \tag{10}$$

where g_1 and g_2 are named as growth speeds. The new stiffness tensor at the mth material point for next analysis of the structure is given as follows:

$$D_{k+1,\,m,\,ijkl} = \rho_{k+1,m}^{p} D_{0,\,ijkl} \tag{11}$$

3.6 Update of SED reference interval

In a stiffness design with volume constraint and/or displacement constraints, it is hard to accurately provide a fixed interval of reference SED for controlling the material distribution of the structure, which satisfies most critical constraint(s) in the optimization process. Therefore, the reference interval of SED changes frequently during the iteration process until the optimal design is obtained. Generally, the length of the reference interval is set to zero to avoid the dependence of the optimal material distribution on the initial parameters. Hence, only the higher bound of the reference interval needs to be updated. The update rule is expressed as follows:

$$\begin{aligned} & u_{\sup}^{ref(k+1)} = \begin{cases} R^{\beta} \cdot u_{\sup}^{ref(k)} & \text{if } R \geqslant 1.0 - \eta \\ R^{\gamma} \cdot u_{\sup}^{ref(k)} & \text{if } R < 1.0 - \eta \end{cases} \\ & \mathrm{Mod}(k, M) = 0 \\ & R = \left(H^{(k)} \Big/ H_0 \right)^{\alpha} \end{aligned} \tag{12}$$

where the exponents $\beta \in [1.0, 2.0]$ and $\gamma \in [10, 30]$ are used in the numerical analysis. The algorithm tolerance is assumed to be $\eta = 1.0$ percent and the integer $M = 4$. $H^{(k)}$ is the current value of the active constraint at kth step and H_0 is the critical value of the corresponding active constraint. $\alpha = 1$ when the active constraint is volume constraint, and $\alpha = -1$ when the active constraint is displacement constraint.

3.7 Optimization procedure

Figure 3 shows the computational procedure of the present algorithm. Generally, the initial relative densities are set to be a positive scalar no more than unity over the whole design domain. In our analysis, the initial supremum of the reference interval is set to be equal to the average SED of the original structure under the specified loading conditions. In iteration, the relative densities are filtered to avoid checkerboard patterns (Sigmund, 2001). The convergence in Step 6 is given as:

$$|R - 1.0| \leqslant \eta \; ; \quad R \in \left\{ R_H^j, \; j = k - N, \cdots, k - 1, k \right\} \tag{13}$$

where integer $N = 15$ is adopted. The maximum iteration ($k_{\max}$) is set to be 100.

4. Results and discussions

In each example, a uniformly fixed finite element mesh is used to describe the geometry and mechanical response within the design domain. The suggested growth

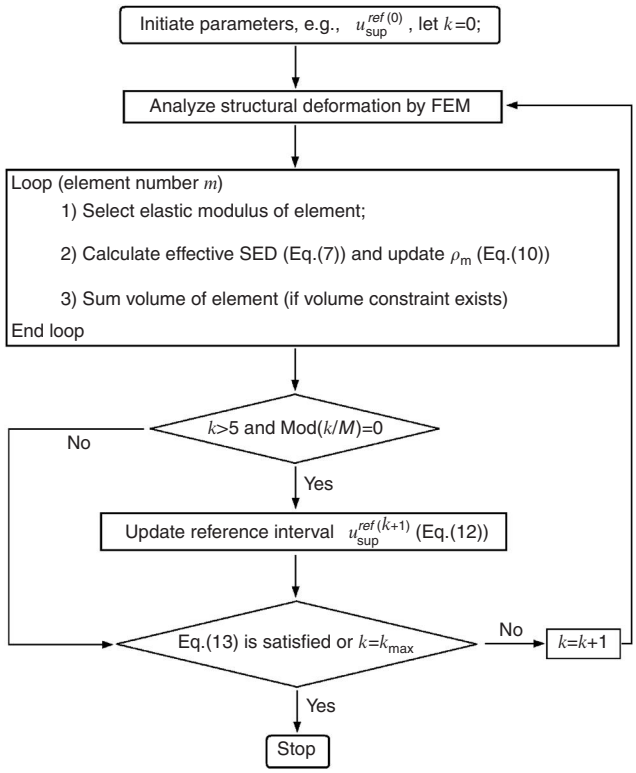

Figure 3.
Flowchart of the present method

speeds $g_1 = 0.8g_2$ and $g_2 \in [0.1, 0.15]$ are used for displacement constraint as an active constraint in the optimization. $g_1 \in [0.1, 0.15]$ and $g_2 = 0.8g_1$ are used for volume constraint (Cai *et al.*, 2008b; Cai and Shi, 2010). In examples, penalization factor $p = 3$.

4.1 Example 1

A 1.0 m × 1.0 m square plate with thickness of 0.005 m is considered in this example (Figure 4(a)). All four sides of the square plate are fixed. A concentrated moment $M_Z = 1.0$ kN.m is applied at the center of the plate which includes bi-modulus material. The higher modulus of the material is 100 GPa and the Poisson's ratio is 0.2. The structure is modeled with 3,600 shell-type finite elements. In the optimization process, the objective is to minimize the structural compliance and the constraint is the final structural volume ratio (the ratio between the current volume and that of the solid structure) is 20 percent. To find the effects of the difference between the tension and compression moduli on the optimal topology designs, three cases are considered: $R_{TCE} = 0.5$; $R_{TCE} = 1.0$; $R_{TCE} = 2.0$.

$R_{TCE} = 0.5$ indicates that the compression modulus equals 100 GPa, while the tension one is 50 GPa. Figure 3(b) displays the final material distribution of the structure in this case. Four arms of the structure are under compression. Near the center of the structure, most material points are under complex stress state, which results in compression modulus of material points. Therefore, the material under compression is used as much as possible in the final structure. $R_{TCE} = 1.0$ implies the material in the initial design exhibiting isotropic, in which the tension modulus is equal to the compression

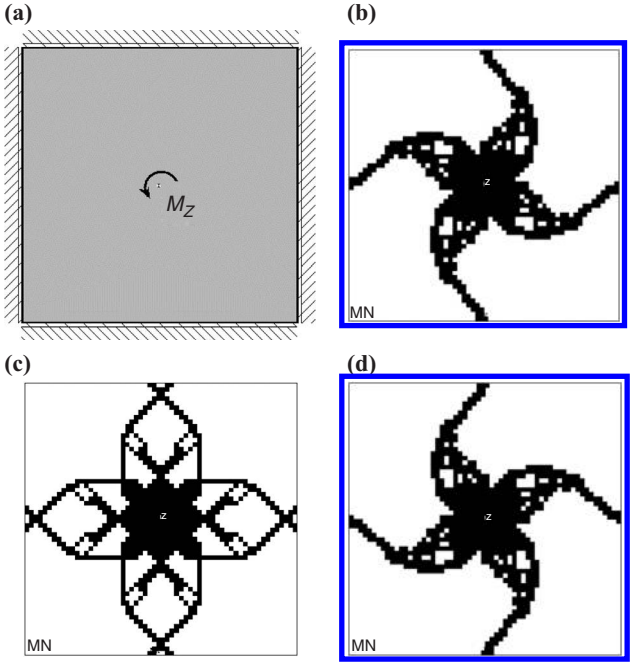

Notes: (a) Initial design; (b) $R_{TCE} = 0.5$; (c) $R_{TCE} = 1.0$ (i.e. isotropic); (d) $R_{TCE} = 2.0$

Figure 4.
Initial and optimal designs under different cases

one. The final topology is given in Figure 4(c), which is both mirror and rotating symmetry. In the optimal structure, the material under compression must be equal to that under tension. $R_{TCE} = 2.0$ means that the tension modulus is higher than the compression modulus (i.e. 50 GPa). Four "arms" of the structure (Figure 4(d)) are under tension, which shows the material with higher modulus is preferable. It can also be fund that the designs in Figure 4(b) and 4(d) show rotating symmetry, which is different from that in Figure 4(c). The structures in Figure 4(b) and 4(d) are identical to each other, i.e. any one of them can be obtained by reflecting the other about *x-z* or *y-z* plane. The conclusion is that the materials with higher modulus are remained as much as possible in the final structures.

Figure 5 shows the histories of structural compliance over iterations for all three cases. For Case 2, the final material distribution is obtained after 49 iterations, and the structural compliance is minimized to 8.63 N.m. For Cases 1 and 3, the optimization process terminated after 45 iterations and their compliances are 8.57 N.m, which is slightly less than that of Case 2. Especially, the structural compliances for Cases 1 and 3 are identical in terms of iterations. The reason is that the structure in the optimization process always shows rotational symmetry.

4.2 Example 2

A MBB beam with size of 3×1 shown in Figure 6 is subjected to a normal concentrated force F at the center of its upper side. The objective is to maximize the stiffness of structure. Volume constraint is considered, e.g. the critical volume ratio is 25 percent. To show the effects of bi-modulus material on final material distribution,

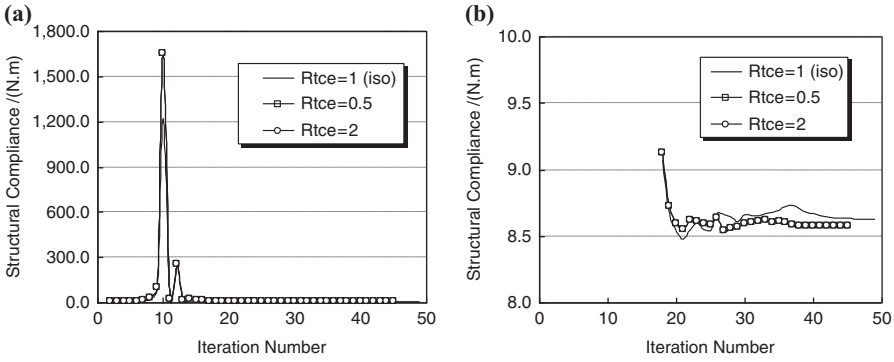

Figure 5.
Iterations of structural compliance for different cases

Notes: (a) Iterations of structural compliance; (b) iteration from step 18

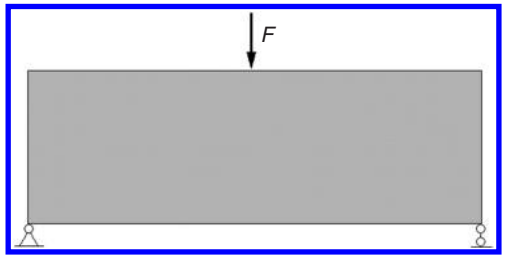

Figure 6.
Initial design of beam and SIMP result

three cases are considered: $R_{TCE} = 1.0$ (isotropic material); $R_{TCE} = 0.01$ (nearly compression only); $R_{TCE} = 100$ (nearly tension only).

Figure 7 shows the final material distribution in structure. Figure 7b shows the isotropic material distribution, which is lightly different from the result (Figure 7(a)) given by SIMP method. Figure 7(c) gives the final bi-modulus material distribution with $R_{TCE} = 0.01$, which implies the compression modulus is far greater than the tension modulus. More material is layout far away from the position with force F. Especially, the two ends of the bottom are not connected with straight line (see Figure 7(a), (b)). Figure 7(d) demonstrates the final material distribution when the tension modulus is far greater than the compression one, e.g. $R_{TCE} = 100$. The structure has two layers of material to bear tension and the two layers are not connected directly. As the load position is far away from the supports, most material are still under compression. From above, the three layouts of bi-modulus materials are different in structure.

4.3 Example 3

The design domain is given in Figure 8(a), which is a 60 m × 71 m rectangular structure with unit thickness (Chang *et al.*, 2007). All four corners of the structure are

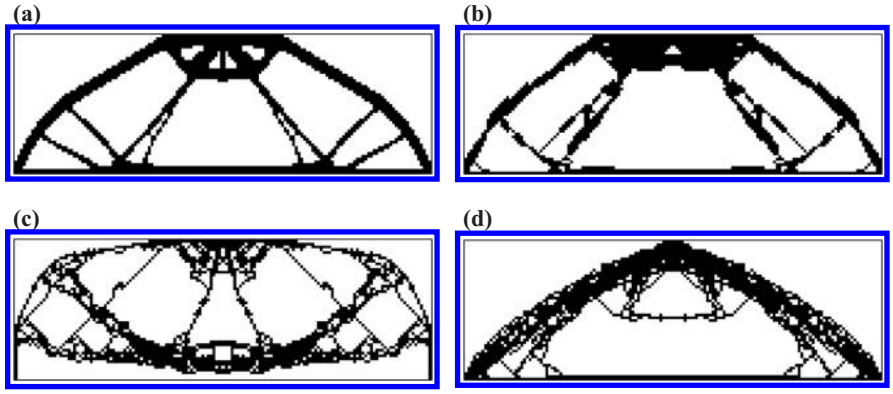

Notes: (a) Material distribution by SIMP method; (b) result of case ($R_{TCE} = 1.0$), i.e. material shows isotropic; (c) result of case ($R_{TCE} = 0.01$), i.e. $0.01E_T E_C$; (d) result of case ($R_{TCE} = 100$), i.e. $E_T = 100\ E_C$

Figure 7.
Optimal topologies of structure with different type of bi-modulus material

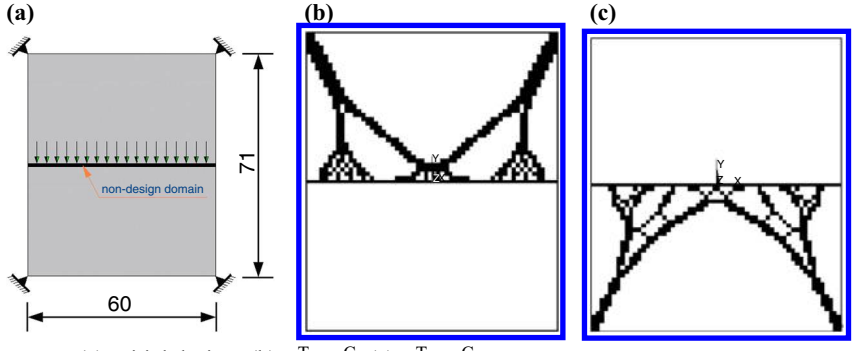

Notes: (a) Initial design; (b) $E^T > E^C$; (c) $E^T < E^C$

Figure 8.
Initial design domain of the structure and the final material distributions for two cases

fixed. A non-design domain at the middle of the structure is assumed and its upper surface is subjected to a uniform pressure of 1,000 Pa. Considering the symmetry of structure, only half of the structure is modeled with 30 × 71 plane stress elements. The bi-modulus material has two moduli 20 and 0.02 GPa, respectively. The Poisson's ratio of the bi-modulus material is assumed to be 0.2. The objective is to minimize the amount of material in the structure, while the maximum deflection of the loading surface is less than or equal to 0.6 mm. Two numerical cases are considered for investigating effects of the difference between the two moduli on the final material distribution of the structure: the tension modulus is 1,000 times of the compression modulus ($R_{TCE} = 1{,}000$); the compression modulus is 1,000 times of tension modulus ($R_{TCE} = 0.001$).

Figure 8(b) displays the material distribution of the optimal structure. The design is symmetry and there is no material in the lower part of the structure. Clearly, all the material in the design domain is subject to tension, and the components like cables to support the non-design domain. The structure more looks like a cable-supported bridge. Figure 8(c) shows the final topology of the structure, in which the material is under compression and the structure is symmetry. The topology is different from that shown in Figure 8(b). The structure looks like an arch bridge. Figure 10 gives the iterative histories of the volume ratios with respect to different types of material from the seventh step. The volume ratio of the final structure, as shown in Figure 8(b), reaches 10.9 percent after 41 iterations. The volume ratio of the structure in Figure 8(c) reaches 7.9 percent after 52 iterations.

The topologies of the structure shown in Figure 9 were given by Chang *et al.* (2007). In their design, the objective is to minimize the structural compliance considering volume constraint, and the material shows tension/compression only. The topologies in Figure 8 are similar to those in Figure 9, which shows the present algorithm is valid. The difference between the proposed results and those by Chang *et al.* (2007) still exists, which is caused by two reasons: first, the optimization models are different, e.g. the present method is to minimize the structural volume with displacement constraint, and second, the other is that the present method to update design variables is heuristic while the method in Chang *et al.* (2007) is sensitivity-based.

Half of the structure has 30 × 71 square elements. Along vertical direction, there are 71 layers and the mid-layer (the 36th layer) is defined as "non-design domain"

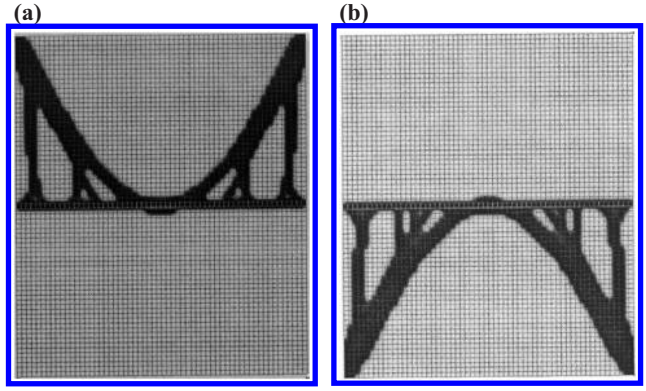

Notes: (a) Tension only design; (b) compression only design
Source: Chang *et al.* (2007)

Figure 9.
The tension/compression only design

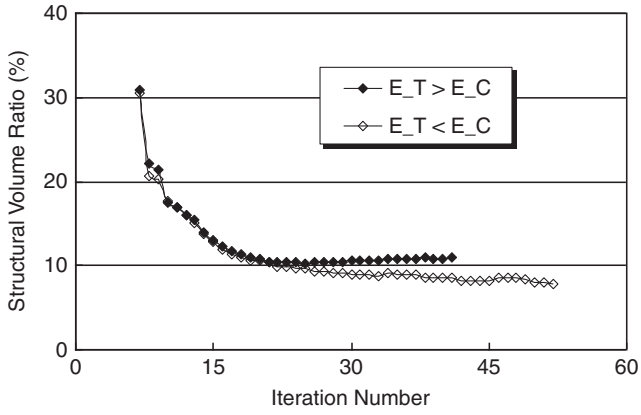

Figure 10.
Iterative history of volume ratios of structure for different cases

(see Figure 8(a)). The uniform pressure is applied on the upper boundary of the layer. Therefore, the model has only vertical mirror symmetry. The difference between Figure 8(b) and 8(c) is caused by the position of the load. One can also find that the difference between Figure 9(a) and 9(b), which is caused by the same reason.

4.4 Example 4

Consider a cube with unit side-length (Figure 11(a)), subjected to a uniform pressure of 1.0 kPa on its top surface. Four corners and four mid-side points on the bottom surface of the structure are fixed along z-direction (which is parallel to the normal of the bottom surface). Considering the symmetry, only a quarter of the structure is modeled in FEM and the component is uniformly divided into 25 × 25 × 50 (X × Y × Z) brick elements, with the bi-modulus material in the design domain ($R_{TCE} = 0.001$). The compression modulus and Poisson's ratio of the material are 20 GPa and 0.2, respectively. The objective is to minimize the amount of material in the structure provided the maximum displacement of the upper surface is less than or equal to 0.02 m. At the same time, the topology optimization of the structure with the isotropic material ($E = 20$ GPa) is analyzed to enable a comparison with the material distribution of the structure with the bi-modulus material.

Figure 11(b) lists the results with isotropic material ($R_{TCE} = 1.0$) after topology optimization. Although the eight points on the bottom surface of the structure are

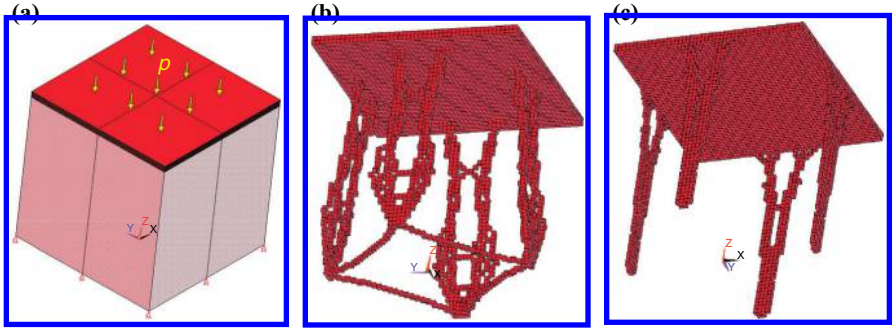

Notes: (a) Initial design; (b) $R_{TCE} = 1.0$; (c) $R_{TCE} = 0.001$

Figure 11.
Initial and optimal topologies of the structure with different values of R_{TCE}

fixed, it is found from Figure 11(b) that there are only four legs under the "desktop," i.e. the non-design domain. These legs are not vertical to the "desktop," and their feet are connected as a whole, which will enhance the global stability of the structure. Obviously, the material connecting these legs is under tension while the legs themselves are under compression. When the ratio R_{TCE} is far less than unity, the material can be approximately considered as compression-only one. Figure 11(c) is the final material distribution of the structure when $R_{TCE} = 0.001$. There are four "legs" of the structure and all the materials in the legs are adjacent to vertical sides. There are mutual connections between legs, which are different from the result in Figure 11(b). So, there is no material under tension in the structure.

4.5 Example 5

A cantilever beam with thickness of 0.01 m shown in Figure 12 is subjected to three concentrated force (100 N) on the upper side. The objective is to maximize the stiffness of structure. Volume constraint is considered, e.g. the critical volume ratio is 40 percent. To show the effects of bi-modulus material on final material distribution, two cases are considered: $R_{TCE} = 1.0$ (isotropic material); $R_{TCE} \neq 1.0$. Although the values of initial growth speeds have been suggested, the effects of growth speeds, i.e. g_1 and g_2 and initial designs ($\rho^{(1)}$ is the initial value of the relative densities of all elements in design domain), on the final distribution of material in structure are discussed in this section, either.

4.5.1 Effects of growth speeds and initial designs on final design. Figure 13 shows the final material distributions in structure with different algorithm parameters. $\rho^{(1)}$ means the initial value of the relative density of an element in design domain.

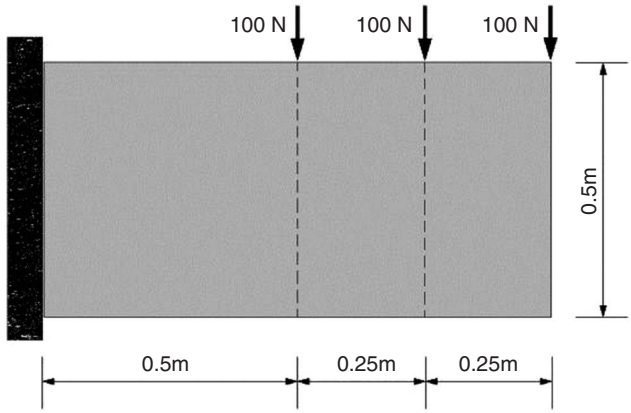

Figure 12.
Initial design of beam

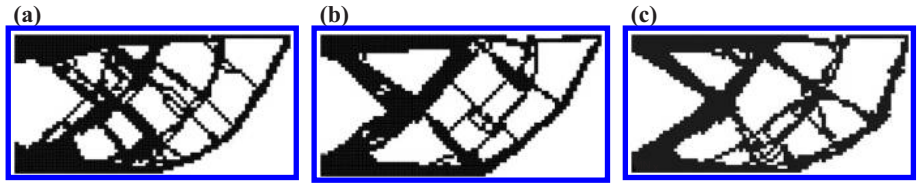

Figure 13.
Optimal topologies of structure with isotropic material but different growth speeds ($g_2 = 1.25g_1$) and initial designs ($\rho^{(1)}$)

Notes: (a) g_1=0.12, $\rho^{(1)}$=0.05; (b) g_1=0.20, $\rho^{(1)}$=0.4; (c) g_1=0.25, $\rho^{(1)}$=1.0

The growth speeds are different for the three cases, and the initial designs are also different. But the differences among the three final material layouts are slight. Therefore, the growth speeds influence the final material layout is slight and the similar conclusion can be found in the work by Cai *et al.* (2008b).

To assess effects of initial design on the final topologies of structure, three typical initial designs are involved in the present study. First, As $\rho^{(1)} = 0.05$, the volume of solid material is only 5 percent of total volume of design domain. After 49 times of iteration, the compliance convergences at 0.02546 N.m (see Figure 14). And the final material layout is shown in Figure 13(a). Second, when the initial design with $\rho^{(1)} = 0.4$, which is equal to the critical value of volume constraint, is specified, the final topology of structure is given in Figure 13(b). The structural compliance approaches 0.02559 N.m after 33 iterations. Third, the initial design can also be specified as the structure filled with solid material, i.e. $\rho^{(1)} = 1.0$. After 31 iterations, the final structural compliance (Figure 13(c)) tends to be 0.02547 N.m. The biggest relative error among the three structural compliances is less than 1 percent. Therefore, the initial design influences the final results slightly, too.

4.5.2 Effect of bi-modulus behavior on final design. In this section, the growth speeds are $g_1 = 0.2$, $g_2 = 0.25$ and the initial design satisfies $\rho^{(1)} = 1.0$.

Figure 15 demonstrates the final bi-modulus material layout in structure by the present method. Clearly, the difference between the two topologies in Figure 15 is

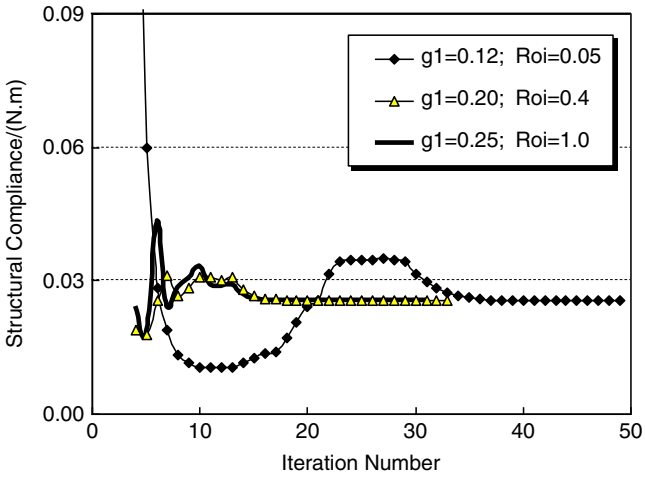

Figure 14.
Iteration histories of mean structural compliance for different cases

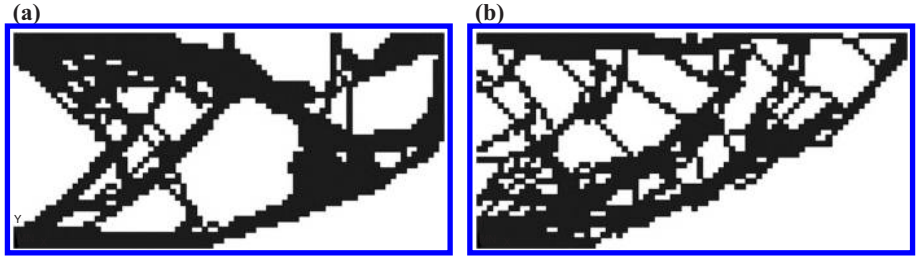

Notes: (a) $R_{TCE} = 0.1$; (b) $R_{TCE} = 10$

Figure 15.
The final bi-modulus material layouts in structure

obvious. As $R_{TCE} = 0.1$, then tension modulus is only 10 percent of the compressive modulus, therefore, the amount of material under tension in Figure 15(a) is greater than that in Figure 15(b) with $R_{TCE} = 10$. Both material layouts in Figure 15 are not similar with those in Figure 13.

5. Conclusions

This paper proposes a bio-inspired topology optimization method for bi-modulus structures using bone remodeling method. Several typical numerical examples are used to show the validity and efficiency of the material-replacement method for the topology optimization of bi-modulus structures. In particular:

(1) The ratio between the tension modulus and the compression modulus of the bi-modulus material in a structure generally has a significant effect on the final topology design, which is different from that in the same structure with isotropic material.

(2) In the optimal structure, it can be found that the material points with the higher modulus are reserved as much as possible.

(3) When the ratio is far more than unity, the material can be considered as tension-only material. If the rate is far less than unity, the material can be considered as compression-only material. As a result, the topology optimization of continuum structures with tension-only or compression-only materials can also be solved by the proposed method.

(4) Algorithm parameters, e.g. growth speeds and initial design, have slight effect on final bi-modulus material layout.

References

Allaire, G., Jouve, F. and Toader, A.M. (2004), "Structural optimization using sensitivity analysis and a level-set method", *Journal of Computational Physics*, Vol. 194 No. 1, pp. 363-393.

Andrade-Campos, A., Ramos, A. and Simões, J. (2012), "A model of bone adaptation as a topology optimization process with contact", *Journal of Biomedical Science and Engineering*, Vol. 5 No. 5, pp. 229-244.

Bagge, M. (2000), "A model of bone adaptation as an optimization process", *Journal of Biomechanics*, Vol. 33 No. 11, pp. 1349-1357.

Bendsøe, M.P. and Kikuchi, N. (1988), "Generating optimal topologies in structural design using a homogenization method", *Computer Methods in Applied Mechanics and Engineering*, Vol. 71 No. 2, pp. 197-224.

Bendsøe, M.P. and Sigmund, O. (1999), "Material interpolation schemes in topology optimization", *Archive of Applied Mechanics*, Vol. 69 Nos 9/10, pp. 635-654.

Cai, K., Chen, B.S. and Zhang, H.W. (2008a), "Topology optimization of continuum structures with materials exhibiting different tensile and compressive properties", *Chinese Journal of Theoretical and Applied Mechanics*, Vol. 40, pp. 646-653.

Cai, K., Chen, B.S., Zhang, H.W. and Shi, J. (2008b), "Stiffness design of continuum structures by a bionics topology optimization method", *Journal of Applied Mechanics – Transactions of the ASME*, Vol. 75, pp. 051001-051011.

Cai, K. and Shi, J. (2010), "A bionic approach for topology optimization for tension-only or compression-only design", *Journal of Bionic Engineering*, Vol. 7 No. 4, pp. 397-404.

Chang, C.J., Zheng, B. and Gea, H.C. (2007), "Topology optimization for tension/compression only design", *Proceedings of the 7th World Congress on Structural and Multidisciplinary Optimization, COEX, Seoul*, pp. 2488-2495.

Cowin, S.C. (1986), "Wolff's law of trabecular architecture at remodeling equilibrium", *Journal of Biomechanical Engineering-Transactions of the Asme*, Vol. 108 No. 1, pp. 83-88.

Eschenauer, H.A. and Olhoff, N. (2001), "Topology optimization of continuum structures: a review", *Applied Mechanics Reviews*, Vol. 54 No. 4, pp. 331-390.

Fernandes, P., Rodrigues, H. and Jacobs, C. (1999), "A model of bone adaptation using a global optimisation criterion based on the trajectorial theory of Wolff", *Computer Methods in Biomechanics and Biomedical Engineering*, Vol. 2 No. 2, pp. 125-138.

Fernandes, P.R., Folgado, J., Jacobs, C. and Pellegrini, V. (2002), "A contact model with ingrowth control for bone remodelling around cementless stems", *Journal of Biomechanics*, Vol. 35 No. 2, pp. 167-176.

Gao, D.Y. (2007), "Solutions and optimality criteria to box constrained nonconvex minimization problems", *J. Industrial and Management Optimization.*, Vol. 3 No. 2, pp. 293-304.

Gao, D.Y. and Ruan, N. (2010), "Solutions to quadratic minimization problems with box and integer constraints", *J. Global Optimization*, Vol. 47 No. 3, pp. 463-484.

Harrigan, T.P. and Hamilton, J.J. (1994), "Bone remodeling and structural optimization", *Journal of Biomechanics*, Vol. 27 No. 3, pp. 323-328.

Huiskes, R., Ruimerman, R., van Lenthe G.H. and Janssen, J.D. (2000), "Effects of mechanical forces on maintenance and adaptation of form in trabecular bone", *Nature*, Vol. 405 No. 6787, pp. 704-706.

Jang, I.G. and Kim, I.Y. (2008), "Computational study of Wolff's law with trabecular architecture in the human proximal femur using topology optimization", *Journal of Biomechanics*, Vol. 41 No. 11, pp. 2353-2361.

Jang, I.G., Kim, I.Y. and Kwak, B.M. (2009), "Analogy of strain energy density based bone-remodeling algorithm and structural topology optimization", *Journal of Biomechanical Engineering*, Vol. 131 No. 1, p. 011012.

Luo, Z., Tong, L.Y., Wei, P. and Wang, M.Y. (2009), "Design of piezoelectric actuators using a multiphase level set method of piecewise constants", *Journal of Computational Physics*, Vol. 228 No. 7, pp. 2643-2659.

Luo, Z., Wang, M.Y., Wang, S. and Wei, P. (2008), "A level set-based parameterization method for structural shape and topology optimization", *International Journal for Numerical Methods in Engineering*, Vol. 76 No. 1, pp. 1-26.

Medri, G. (1982), "A non-linear elastic model for isotropic materials with different behavior in tension and compression", *Journal of Engineering Materials and Technology*, Vol. 104 No. 1, pp. 26-28.

Mullender, M.G., Huiskes, R. and Weinans, H. (1994), "A physiological approach to the simulation of bone remodeling as a self-organizational control process", *Journal of Biomechanics*, Vol. 27 No. 11, pp. 1389-1394.

Qin, Q.H. (2003), "Variational formulations for TFEM of piezoelectricity", *International Journal of Solids and Structures*, Vol. 40, pp. 6335-6346.

Qin, Q.H. (2005), "Trefftz finite element method and its applications", *Applied Mechanics Reviews*, Vol. 58 No. 5, pp. 316-337.

Qin, Q.H. (2007), "Multi-field bone remodeling under axial and transverse loads", in Boomington, D.R. (Ed.), *New Research on Biomaterials*, Nova Science Publishers, New York, NY, pp. 49-91.

Qin, Q.H. and He, X.Q. (2005), "Variational principles, FE and MPT for analysis of nonlinear impact contact problems", *Computer Methods in Applied Mechanics and Engineering*, Vol. 122 Nos 3/4, pp. 205-222.

Qin, Q.H. and Ye, J.Q. (2004), "Thermoelectroelastic solutions for internal bone remodeling under axial and transverse loads", *International Journal of Solids and Structures*, Vol. 41, pp. 2447-2460.

Qin, Q.H., Qu, C.Y. and Ye, J.Q. (2005), "Thermo electroelastic solutions for surface bone remodeling under axial and transverse loads", *Biomaterials*, Vol. 26 No. 33, pp. 6798-6810.

Qu, C.Y. and Qin, Q.H. (2006), "Evolution of bone structure under axial and transverse loads", *Structural Engineering and Mechanics*, Vol. 24 No. 1, pp. 19-29.

Qin, Q.H. and Wang, H. (2008), *Matlab and C Programming for Trefftz finite Element Methods*, Taylor & Francis, Boca Raton, FL.

Qu, C.Y., Qin, Q.H. and Kang, Y.L. (2006), "A hypothetical mechanism of bone remodeling and modeling under electromagnetic loads", *Biomaterials*, Vol. 27 No. 21, pp. 4050-4057.

Sigmund, O. (2001), "A 99 line topology optimization code written in Matlab", *Structural and Multidisciplinary Optimization*, Vol. 21 pp. 120-127.

Wang, M.Y., Wang, X.M. and Guo, D.M. (2003), "A level set method for structural topology optimization", *Computer Methods in Applied Mechanics and Engineering*, Vol. 192 pp. 227-246.

Wolff, J. (1986), "The law of bone remodeling", (Edited and Trans by P. Maquet and R. Furlong), *Das Gesetz der Transformation der Knochen*, Springer, Berlin, Heidelberg, New York, NY.

Xie, Y.M. and Steven, G.P. (1993), "A simple evolutionary procedure for structural optimization", *Computers and Structures*, Vol. 49 No. 5, pp. 885-896.

Zhou, M. and Rozvany, G.I.N. (1991), "The COC algorithm, Part II: topological, geometry and generalized shape optimization", *Computer Methods in Applied Mechanics and Engineering*, Vol. 89 Nos 1/3, pp. 197-224.

Corresponding author
Professor Qing H. Qin can be contacted at: qinghua.qin@anu.edu.au